

APPENDIX 12

DIXIE VALLEY WELLFIELD CROSS-SECTIONS WITH ASSUMPTIONS

Table of Contents

Introduction.....	3
Cross-Section Index Map.....	3
Primary Assumptions.....	5
A-A'.....	6
B-B'.....	6
C1-C1'.....	7
D-D'.....	7
E-E'.....	7
F-F'.....	7
G-G'.....	8
H-H'.....	8
Cross-Section Legend.....	9
Cross-Section A-A'.....	10
Cross-Section B-B'.....	10
Cross-Section C1-C1'.....	11
Cross-Section C-C'.....	11
Cross-Section D-D'.....	12
Cross-Section E-E'.....	12
Cross-Section F-F'.....	13
Cross-Section G-G'.....	13
Cross-Section H-H'.....	14

Dixie Valley Baseline Conceptual Geothermal Model

Wellfield Cross-Sections

Introduction

Nine cross-sections have been constructed through the Dixie Valley wellfield (Figure 1). Six of the nine cross-sections, specifically A-A' through F-F', were quantitatively analyzed using various geostatistical methods, while all the sections were used for qualitative analysis, creation of the baseline conceptual model, and application for EGS favorability mapping. Information within the cross-sections utilize well data as the main control points including the known lithology and thermal data. Other factors taken into account were the surface geology, gravity and magnetic surveys (to infer depth to the basement, basin profile, and intrabasin faults), and seismic profiles (to infer faulting, depth of basin sediments, and depth to prominent reflectors). The Smith and Blackwell (2001) structure map (Figure 2) provided a template for inferring significant intrabasin faults and a Dixie Valley geophysical basement configuration model was used to constrain the depth of basin-filling sediments (Figure 3). Generic cross-sections provided by Blackwell were weighed heavily into these sections (see main body of text and Figures 4a and 4b). Detailed cross-sectional figures from Gabe Plank's work at the University of Nevada Reno held by the Great Basin Geothermal Center were also incorporated (2002 Dixie Valley Geothermal workshop).

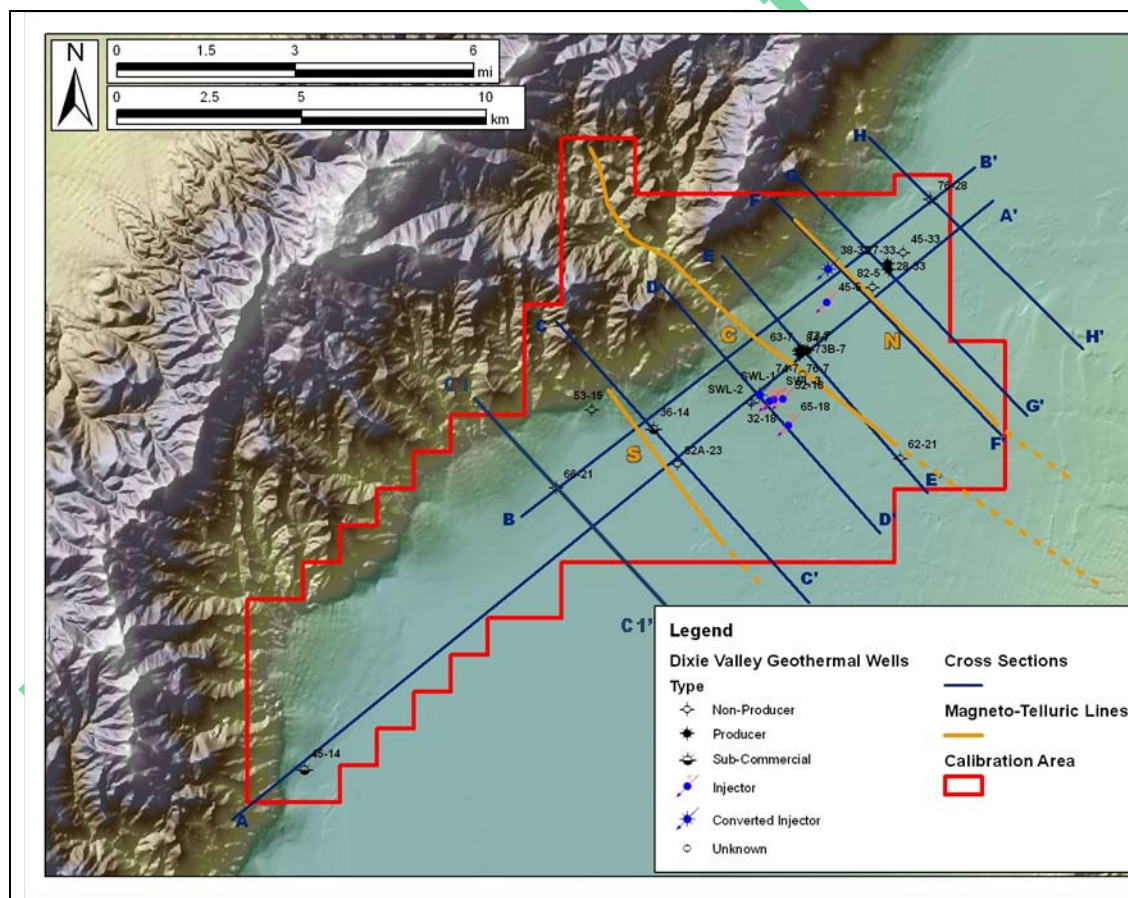


Figure 1. Index map for Dixie Valley with the nine cross-section line locations used in this report. Map produced by Matthew Clyne using GIS.

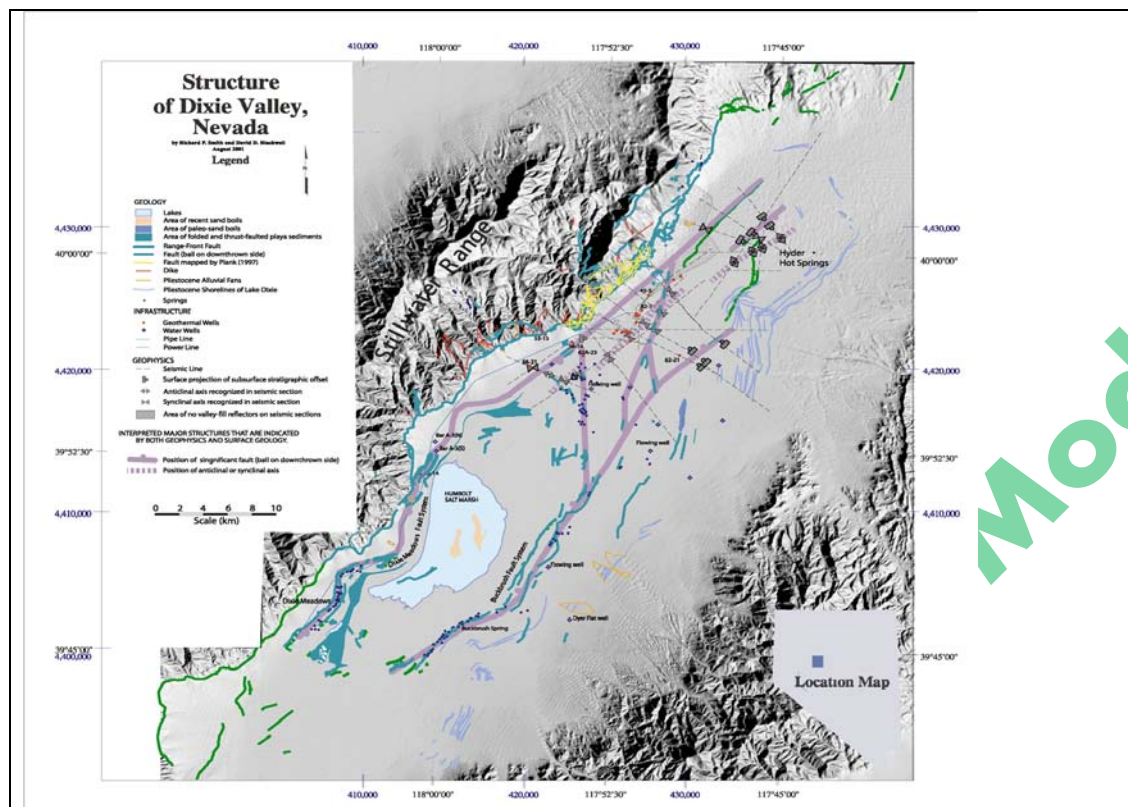


Figure 2. Structure of Dixie Valley from Smith and Blackwell (2001); thick purple lines indicate the positions of interpreted major intrabasin faults based on geophysical data and surface geology.

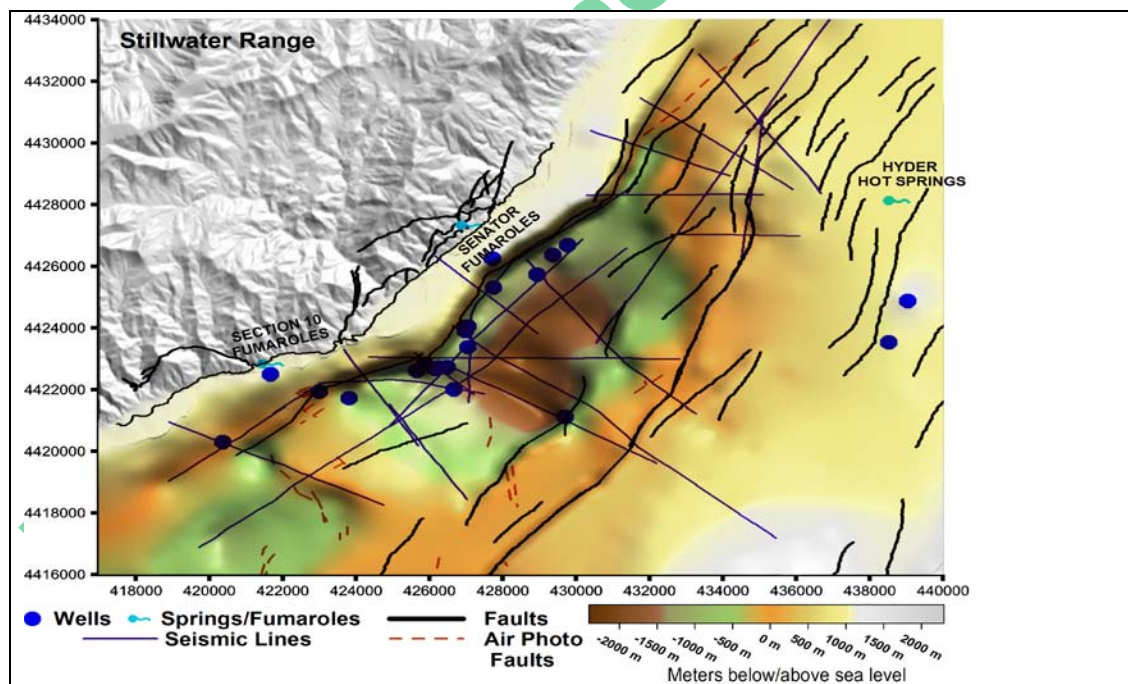


Figure 3. Dixie Valley basement configuration with valley fill removed based on seismic and well data using fault lines to limit contours; from Blackwell et al. (2005).

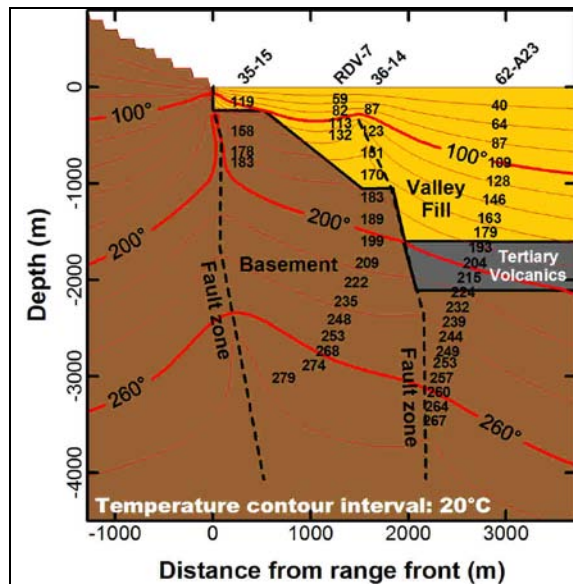


Figure 4A. Thermal model for the DVPP area based on temperature matching in the deep wells (Blackwell et al., 2000).

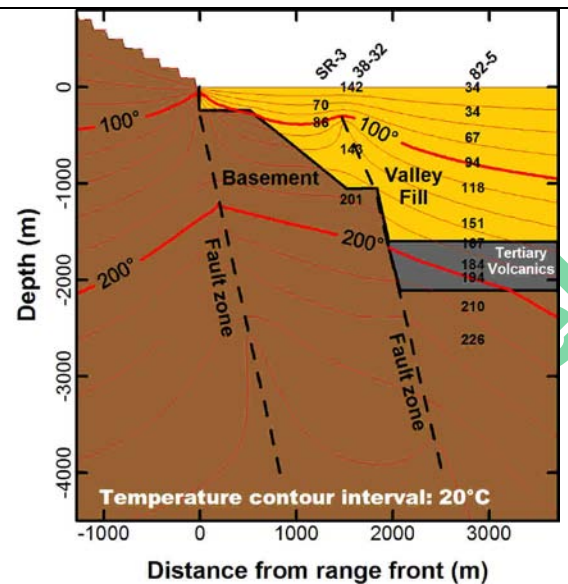


Figure 4B. Thermal model for the DVPP in section 32/33 based on temperature matching in the deep wells (Blackwell et al., 2000).

Well elevation, total depth, and lithology were extracted from public domain geothermal well databases, proprietary logs provided by Al Waibel with the permission of Terra-Gen Corporation, University of Nevada Reno, and well data provided directly from Terra-Gen Corporation. Thermal data was extracted mostly from the SMU online geothermal database. Well temperature data was obtained from temperature-depth profiles provided in Blackwell et al. (2005). See appendix 10 for a generalized description of the available subsurface well lithology subdivided into six stratigraphic units as described in the main body of this report. The depths and intervals in this table represent the depths and formation thicknesses used in the cross-sections.

Primary Assumptions

- The cross sections have no vertical exaggeration and use a meter scale.
- The grid system overlain on the sections are composed of 500m by 500m cells used for qualitative and quantitative analysis.
- The intersection points of the six main wellfield cross sections are labeled at the surface.
- The sections have been divided into six stratigraphic units to be comparable to Blackwell's geologic model presented in the main body of the text:
 - Tbf: basin-filling sediments and lowermost tuffaceous sediments;
 - Tmb: Miocene basalt;
 - Tv or Tvs: Oligocene silicic volcanics, volcaniclastic and lacustrine sediments;
 - Jz igneous section: Jurassic mafic igneous rocks;
 - Jz-Tr section: Jurassic and Triassic meta-sediments; and
 - Kgr: Cretaceous granodiorite (crystalline basement).
- While the Jz Boyer Ranch quartzite has been incorporated into the Tr-Jz meta-sediments stratigraphic unit, it has proven difficult to lump these units. Where the quartzite could not be included in this unit, it has been divided out and labeled Jbr.

- The topographic profile was inferred from well elevations and topographic maps.
- The axis of a syncline within the basin-fill sediments is from seismic data with the approximate location taken from Smith and Blackwell's (2001) structure map.
- If there was no data or structural control on the range-front/piedmont faults, a 75° SE dip was assumed. All of the intra-basin faults are assumed to have a steep dip, while the N-trending geophysical-inferred faults identified in the valley are shown as vertical structures.
- Crystalline basement (Kgr) is assumed to underlie the entire area at some depth in an idealized model (see Figures 2 and 3 within the main report). Idealized contacts with question marks infer where this contact is. At times this contact represents the Dixie Valley fault and/or the piedmont fault, both of which comprise the Dixie Valley fault zone (DVFZ).

Section A-A'

- Well 62-A23 has no lithology data available, so the contact of the Tertiary volcanics was taken from Blackwell's generic thermal model (Figure 4A) where the depth interval is approximately 1.6-2.1 km.
- A basement high was imaged in the seismic data north of 62-A23.
- The piedmont fault is oblique to the cross section line and the offset is unknown.
- The N-trending segment of the range-bounding fault that intersects the cross section near 45-14 must have a steep to near-vertical dip as the structure was not encountered by 45-14. In addition the NE-trending segment of the range-bounding fault at this location (near Dixie Meadows) and to the south have shallow interpreted dips of ~35° SE at Dixie Meadows and 25-30° SE ~ 10 km south of Dixie Meadows based on seismic studies. It is unknown how this interpreted low angle segment connects with the overall steep nature of the fault zone near the producing field.
- The range-bounding fault encountered in this cross section likely inherits an early NS oriented normal fault that has been re-activated in the current extensional phase. This fault segment appears to have an apparent strike-slip sensed motion.
- Similar strike to seismic line 101/8: used to infer basement depth between wells.
- A significant NS oriented fault near well 62-A23 could not be projected at depth as the dip and offset is unknown. This orientation would likely have a strike-slip component in the current stress regime and laterally offsets a syncline axis within the basin-fill sediments.
- The stratigraphy between 45-14 and 62-A23 is unknown and largely inferred.

Section B-B'

- Cross section images the stranded block between the range-bounding and piedmont fault.
- The section runs parallel to these structures and crosses the piedmont fault at a low angle. The exact offset at this intersection is interpreted with an assumed steep apparent dip.
- Within section 33: temperature extracted from 45-33 while the lithology used is from 28-33.
- Basement depth between wells inferred using seismic lines SRC-1, SRC-1N, and 9.
- Well 36-14 did not intersect the Tertiary volcanics but instead encountered basement at ~1 km.
- The range-bounding fault at some depth should be intersected by this section line as shown.

- The stratigraphy of 66-21 is known while 36-14 is inferred from Blackwell's idealized cross-sections.

Section C1-C1'

- Assumes multiple faults comprise the DVFZ in the area SW of the DVPP.
- Dextral strike-slip component on north-trending fault (Blackwell and Smith, 2001).
- Depth of basin-fill derived from geophysical data (Figure 3).
- NW-dipping antithetic faults in the valley imaged by seismic and magnetic data.

Section C-C'

- Wells 36-14 and 62-A23 are deviated towards the range-front at an unknown angle.
- Easternmost antithetic fault imaged by seismic and magnetic data.
- Intrabasin faults (from Smith and Blackwell's 2001 map and shown in Figure 2) are projected within the section and shown as vertical structures as the dip directions are not largely constrained.
- Lithology and thermal data inferred from Blackwell's thermal cross-section (Figure 4A).
- Cross section runs at a slight angle to seismic line 10/105.
- N-trending intrabasin fault is interpreted to be truncated by the piedmont fault near 62-23.

Section D-D'

- Sunoco mud logs provide evidence for a fault zone at 2.25km and 2.43-2.46 km in SWL-2.
- Antithetic fault derived from Plank's cross section and fault zones encountered by drilling.
- Surface intrabasin faults derived from Smith and Blackwell's 2001 map (Figure 2).
- Major intrabasin fault near 62-21 is derived from seismic and geophysics.

Section E-E'

- Basement inferred from seismic line 6.
- Section extends through the deepest part of basin (early NS oriented graben).
- Antithetic fault in producing zone: fault zone logged in section 7 wells.

Section F-F'

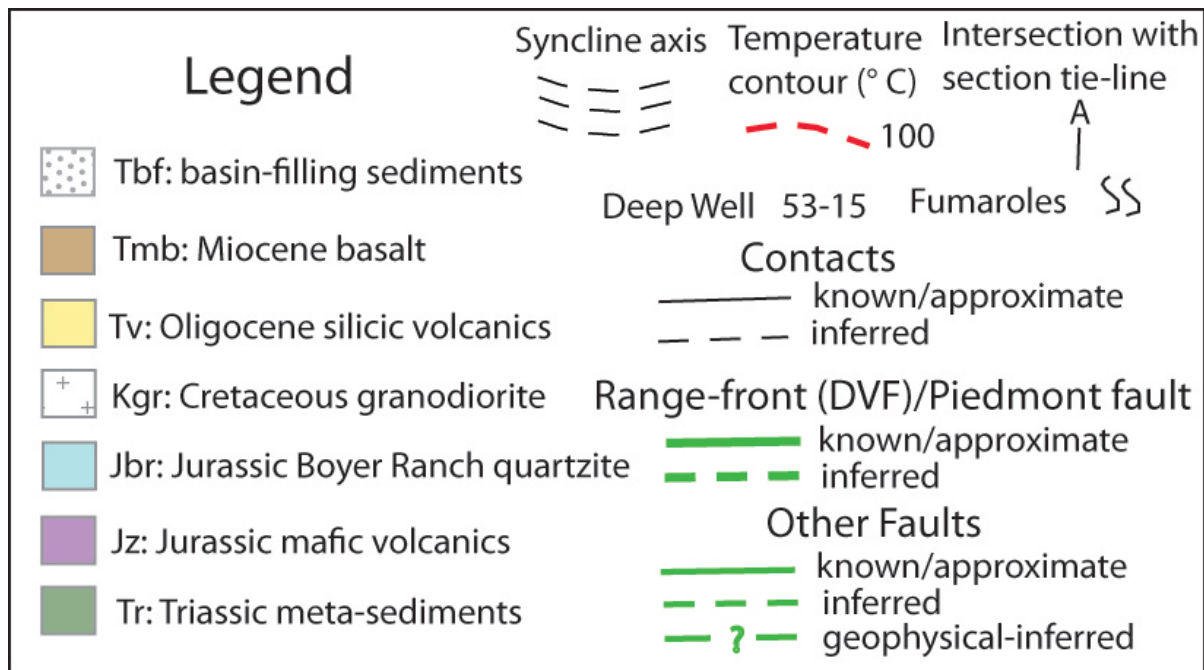
- 38-32: stranded shallow block between main strands of the DVFZ.
- 38-32: brecciated fault zone at a depth of ~1006-1113 meters assumed to be main range front (Johnson and Hulen, 2002) is interpreted as a more north-striking subsidiary strand of the DVFZ.
- 82-5: bottom of well intersects piedmont fault and the footwall block consisting of Kgr.
- 45-5: This well lies off of the cross section plane so the stratigraphy was not used.
- Major intrabasin fault (from Figure 2) intersects the cross section near the piedmont fault.
- Inferences from seismic line SRC-3 and 102.

Section G-G'

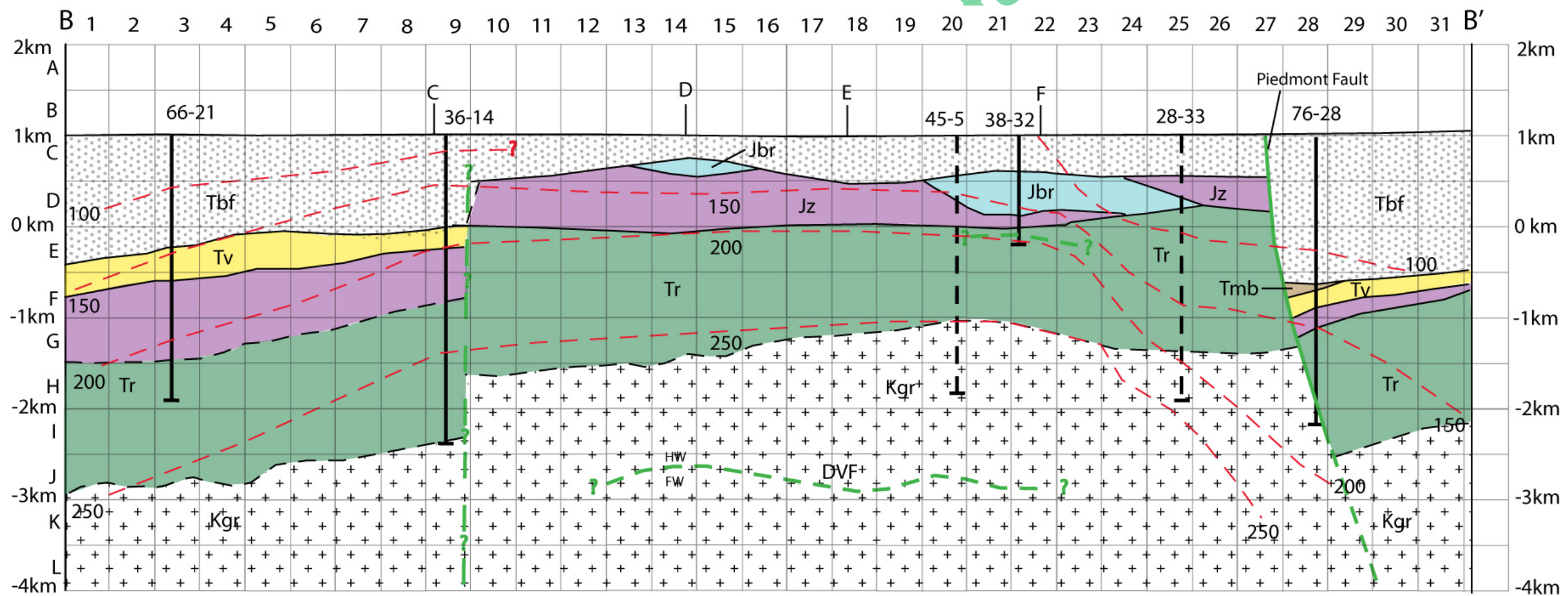
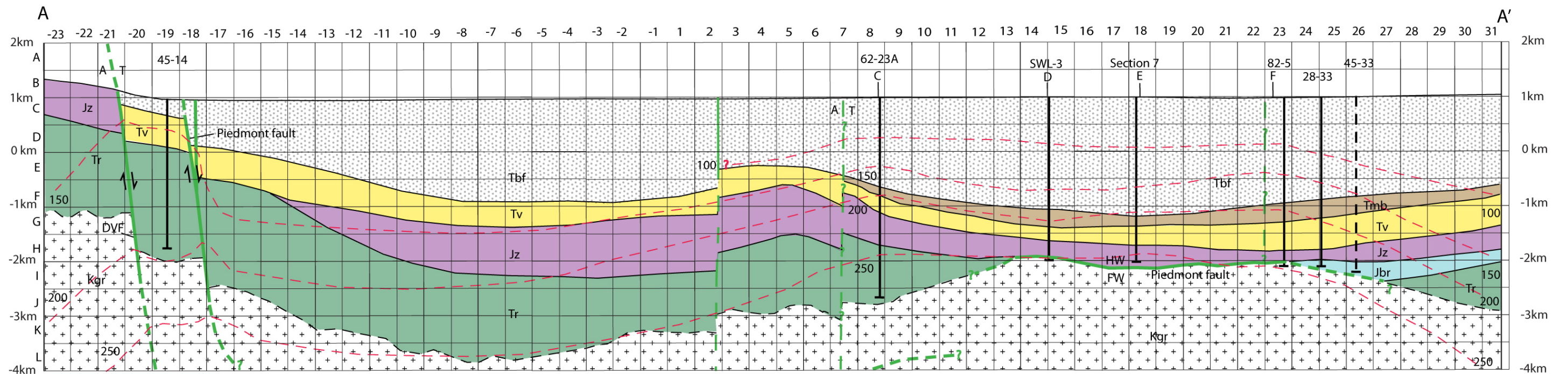
- Jurassic rocks thin (pinch-out) north of the producing field as evidenced by well data, geologic mapping of the Fencemaker and Boyer Thrusts (labeled BT on cross-section), reduced magnetic signature, general map of the Jurassic Lopolith by Wallace and Whitney (1985).
- The schematic of the Jurassic mafic rocks and the Boyer Ranch quartzite in the block between the range-front and piedmont fault is interpretive, but consistent with the lithology from 38-32.
- Producing wells 37-33 and 28-33 intersect the fractured Jurassic rocks in the hanging wall block of the piedmont fault.
- Inferences from seismic reflection line SRC-3 for basement depth in valley.
- Westward dipping faulting bounding the eastern segment of Dixie Valley is derived from the magnetic-gradient and seismic inferred faults (Figure 3).

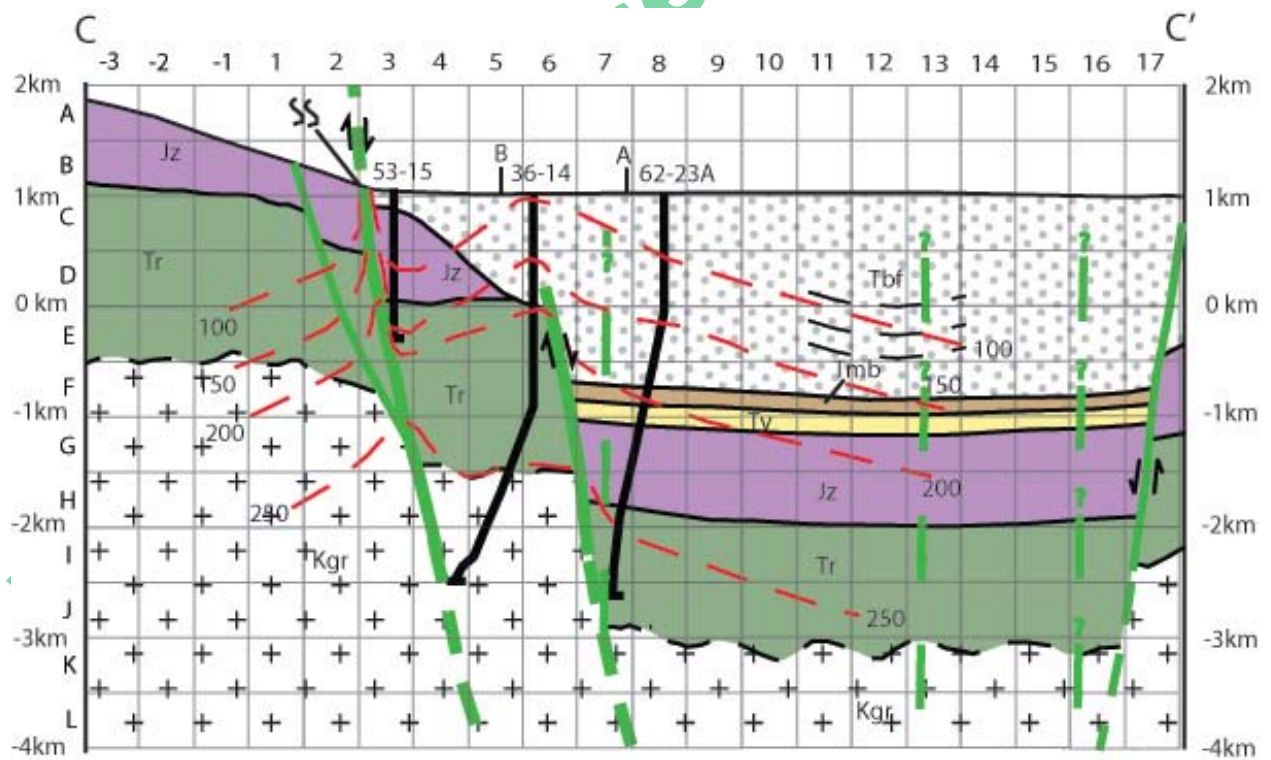
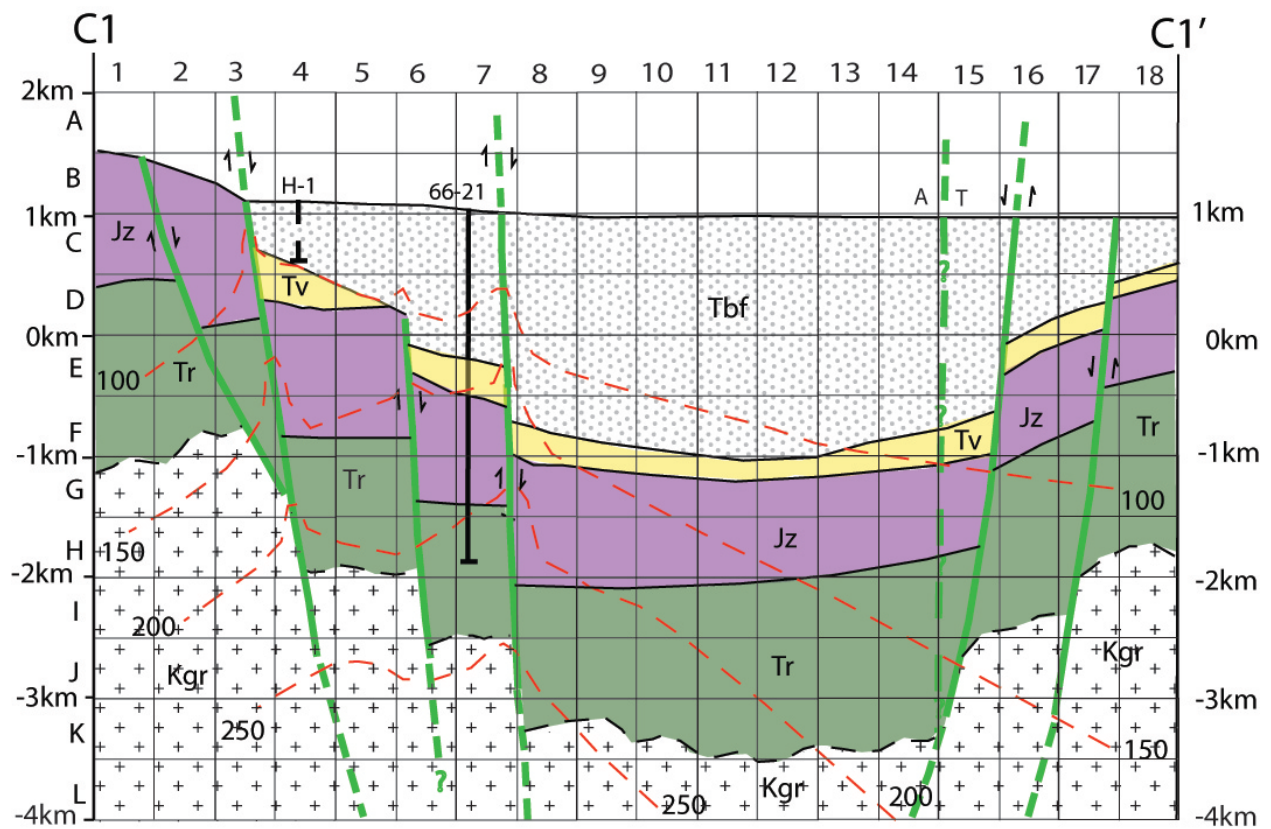
Section H-H'

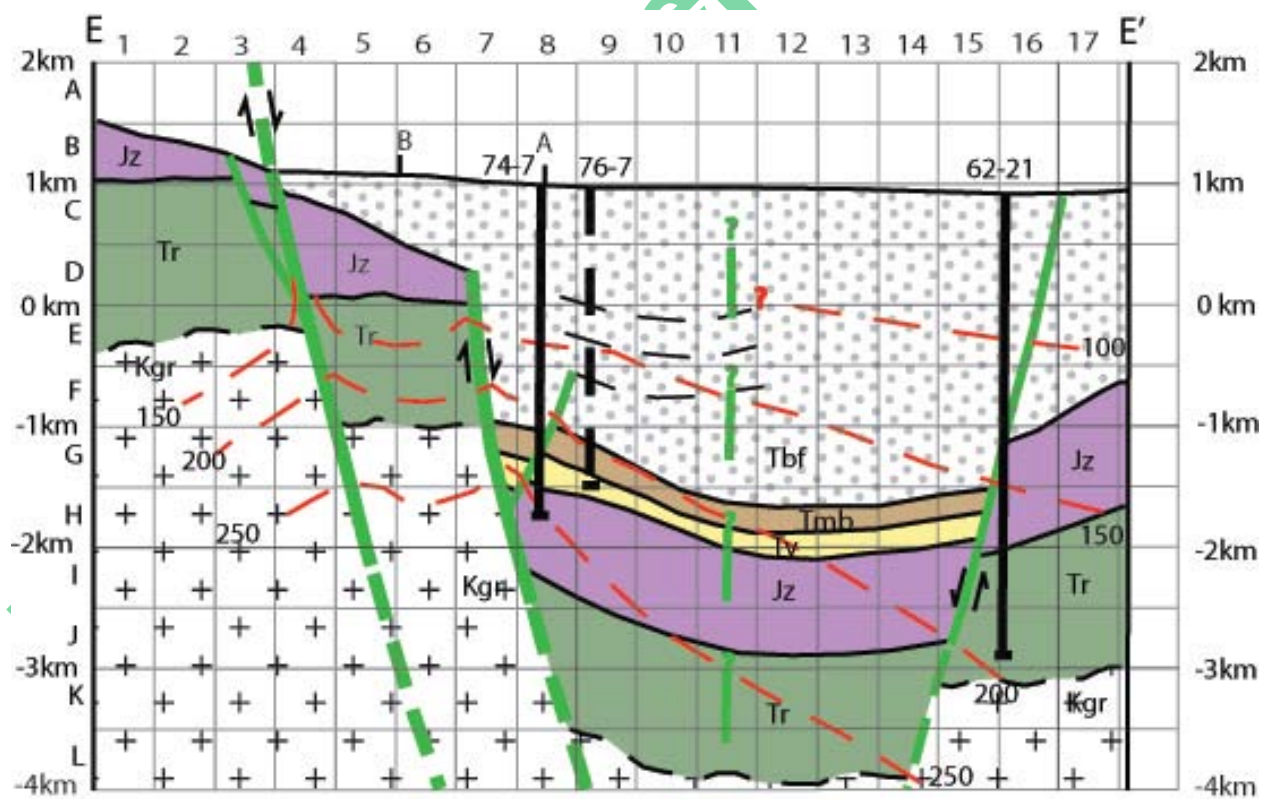
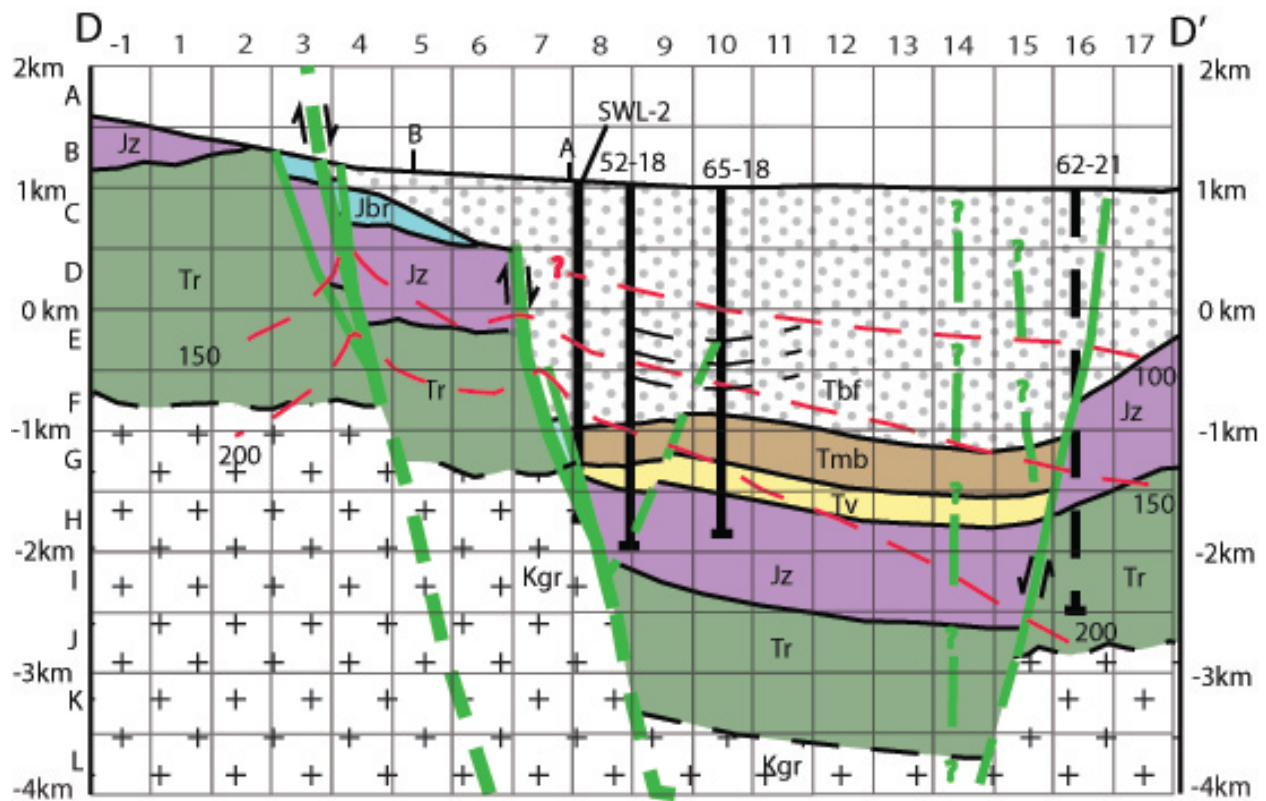
- Major displacement along the piedmont fault is distributed along several faults as evidenced by the surface faulting, geophysical-inferred faulting, and proprietary seismic reflection data provided by Terra-Gen Corp.
- Well 76-28 is a dry, relatively cold well, that doesn't intersect the major piedmont fault.
- Inferences for basement depth and intra-valley faulting derived from proprietary seismic reflection data provided by Terra-Gen Corp.
- Miocene basalt (Tmb) nearly pinches at this point north of the DVPF, as evidenced by lithology found in 76-28.
- The approximate position of the Fencemaker Thrust (FT) is labeled on the section.

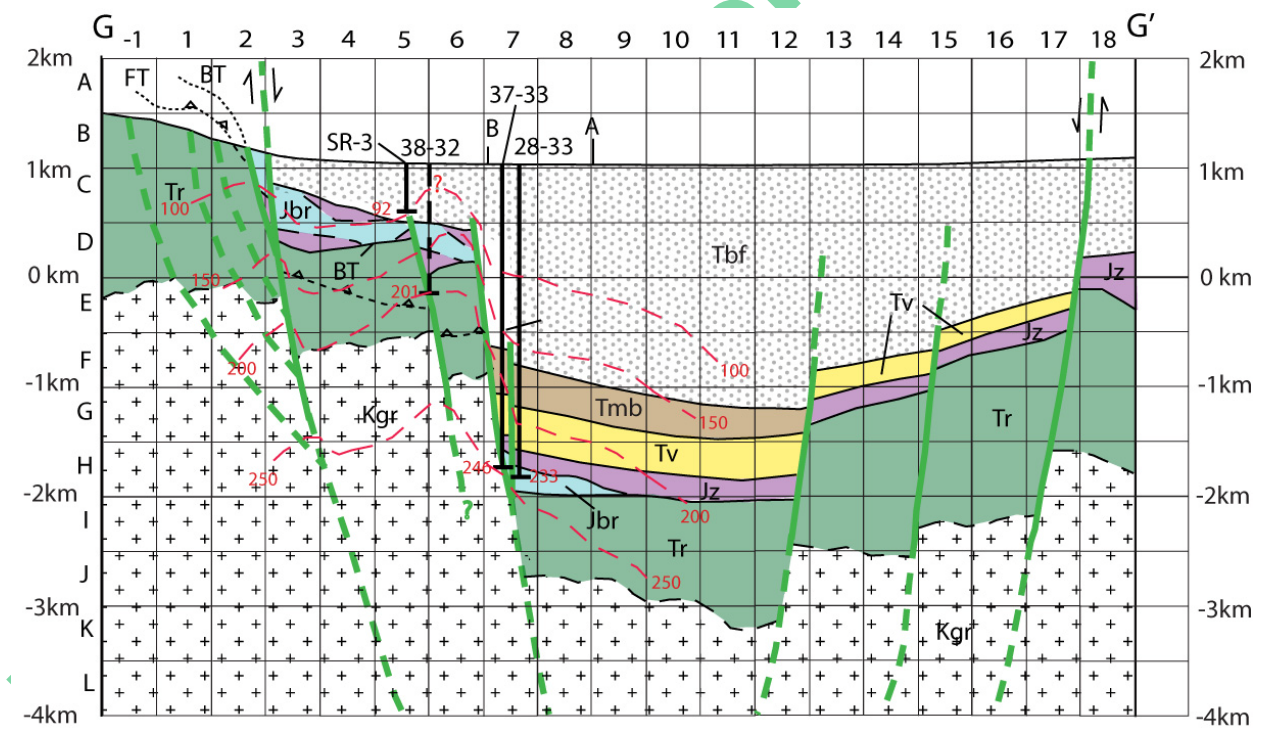
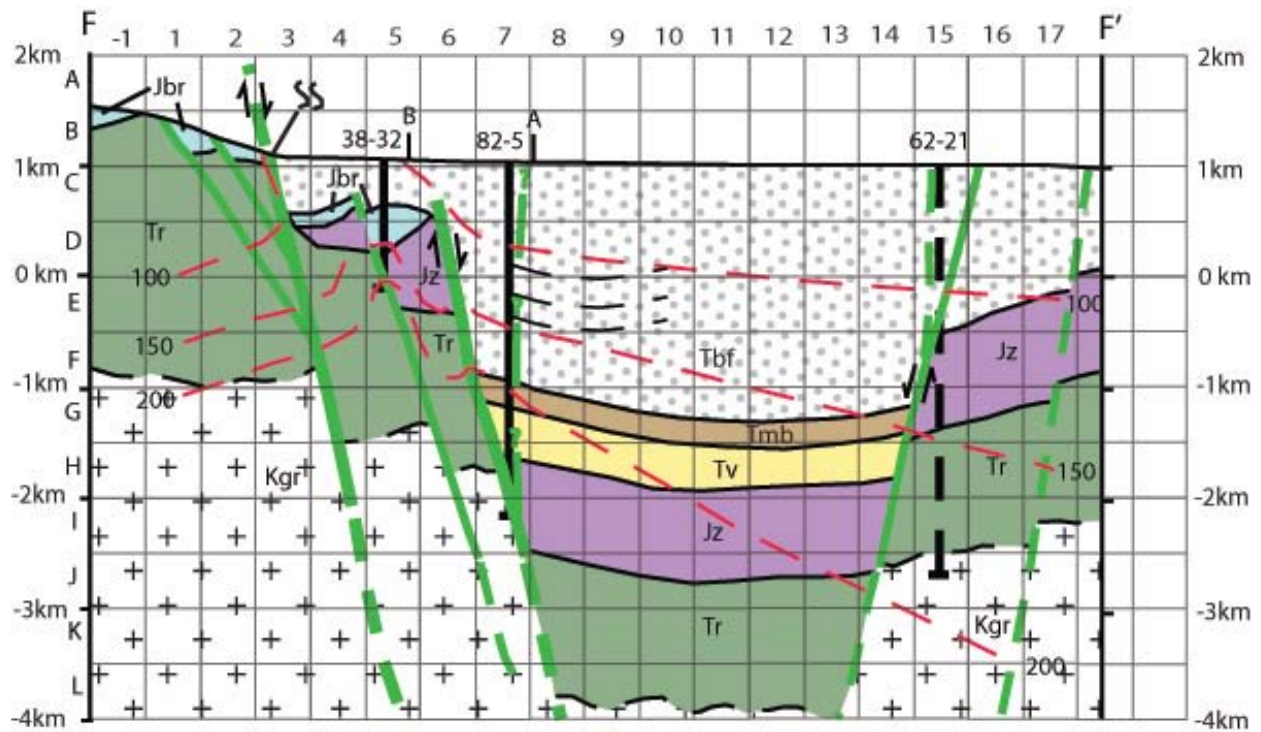


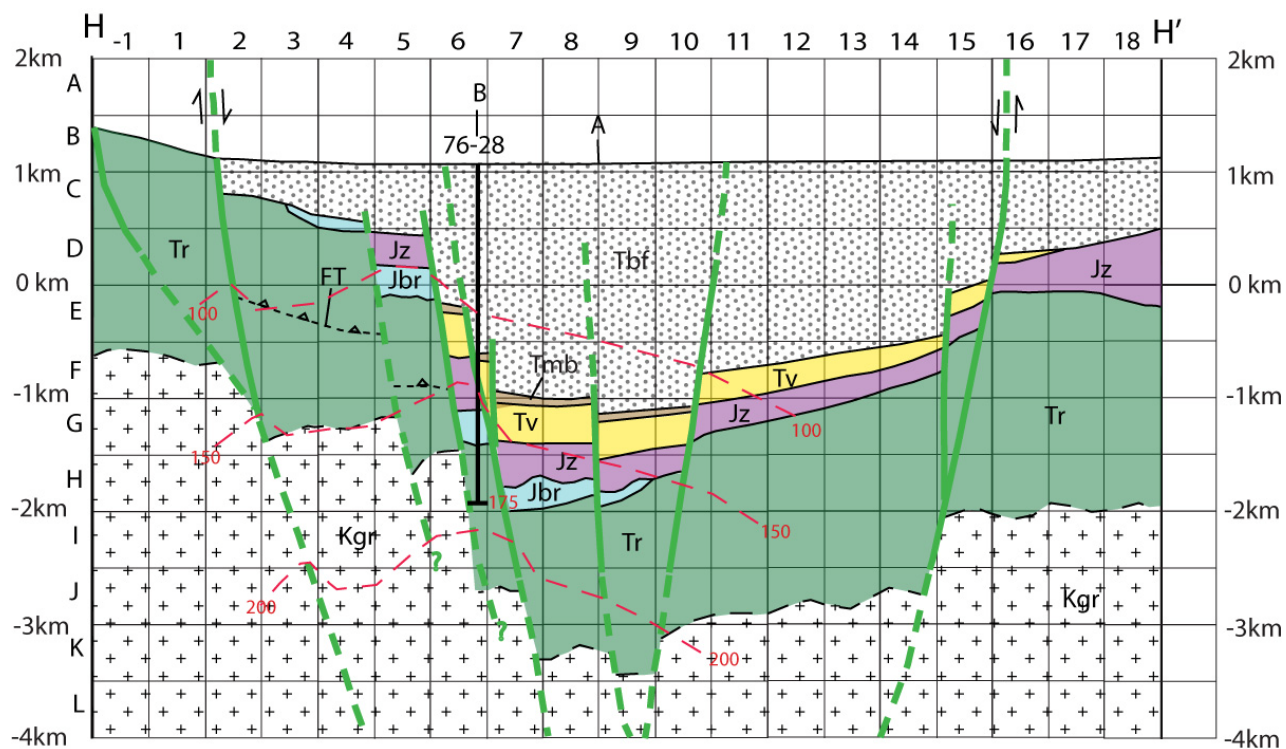
Baseline Conceptual











Baseline Concept